Article

Cell Reports

Enhancer SINEs Link Pol III to Pol II Transcription in Neurons

Graphical Abstract

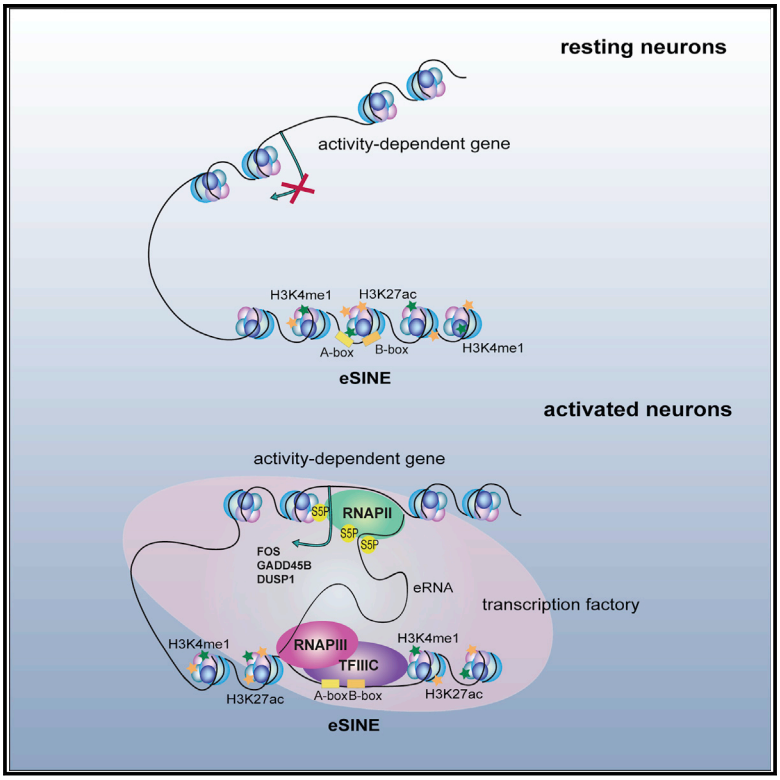

Highlights

- eSINEs share chromatin marks with other neuronal enhancers
- eSINEs are transcribed by Pol III in response to neuronal depolarization
- eSINEs provide a molecular link between Pol III and Pol II transcription
- The eSINE Fos^{RSINE1} controls *Fos* expression during neuronal differentiation

Authors

Cristina Policarpi, Luca Crepaldi, Emily Brookes, Justyna Nitarska, Sarah M. French, Alessandro Coatti, Antonella Riccio

Correspondence

a.riccio@ucl.ac.uk

In Brief

Spatiotemporal regulation of gene expression requires the interaction between promoters and distally located enhancers. Policarpi et al. identify a subset of SINEs that functions as enhancers for activity-dependent neuronal genes. The enhancer SINE Fos^{RSINE1} regulates *Fos* transcription and is necessary for both activity-dependent dendritogenesis and proper brain development.

Data and Software Availability

GSE75191

Policarpi et al., 2017, Cell Reports *21*, 2879–2894
December 5, 2017 © 2018 The Authors.
https://doi.org/10.1016/j.celrep.2017.11.019

CellPress

Cell Reports
Article

OPEN ACCESS
CellPress

Enhancer SINEs Link Pol III to Pol II Transcription in Neurons

Cristina Policarpi,[1] Luca Crepaldi,[1,2,3] Emily Brookes,[1,2] Justyna Nitarska,[1] Sarah M. French,[1] Alessandro Coatti,[1] and Antonella Riccio[1,4,*]
[1]MRC Laboratory for Molecular Cell Biology, University College London, London WC1E 6BT, UK
[2]These authors contributed equally
[3]Present address: Wellcome Genome Campus Hinxton, Wellcome Trust Sanger Institute, Cambridge CB10 1SE, UK
[4]Lead Contact
*Correspondence: a.riccio@ucl.ac.uk
https://doi.org/10.1016/j.celrep.2017.11.019

SUMMARY

Spatiotemporal regulation of gene expression depends on the cooperation of multiple mechanisms, including the functional interaction of promoters with distally located enhancers. Here, we show that, in cortical neurons, a subset of short interspersed nuclear elements (SINEs) located in the proximity of activity-regulated genes bears features of enhancers. Enhancer SINEs (eSINEs) recruit the Pol III cofactor complex TFIIIC in a stimulus-dependent manner and are transcribed by Pol III in response to neuronal depolarization. Characterization of an eSINE located in proximity to the *Fos* gene (Fos^{RSINE1}) indicated that the Fos^{RSINE1}-encoded transcript interacts with Pol II at the *Fos* promoter and mediates *Fos* relocation to Pol II factories, providing an unprecedented molecular link between Pol III and Pol II transcription. Strikingly, knockdown of the Fos^{RSINE1} transcript induces defects of both cortical radial migration *in vivo* and activity-dependent dendritogenesis *in vitro*, demonstrating that Fos^{RSINE1} acts as a strong enhancer of *Fos* expression in diverse physiological contexts.

INTRODUCTION

All organisms respond to environmental conditions by modifying gene expression in a manner that is strictly regulated both temporally and spatially. Although this adaptive response is of fundamental importance for any cell type, it is particularly relevant to neurons. Failure to rapidly adapt the transcriptional output to ever-changing conditions compromises most brain tasks, including learning and memory formation (Flavell and Greenberg, 2008; Sweatt, 2016; West and Greenberg, 2011).

In eukaryotic cells, three RNA polymerases regulate the transcription of largely non-overlapping sets of genes. RNA polymerase II (Pol II) transcribes protein-coding genes, and Pol I and Pol III transcribe rRNA and tRNA genes, respectively (Roeder, 1996). Pol III also transcribes the 5S rRNA, small RNAs, microRNAs, and RNAs derived from DNA-repetitive elements such as short interspersed nuclear elements (SINEs) (Dieci et al., 2007). Despite the fact that most genes transcribed by Pol III are highly conserved across species, the genomic occupancy of the Pol III complex varies greatly between organisms and between cell types within the organism (Barski et al., 2010; Moqtaderi and Struhl, 2004; Moqtaderi et al., 2010; Raha et al., 2010), implying that it may have additional, cell-specific functions. In human cells, Pol III complexes bind preferentially to genomic regions adjacent to Pol II transcriptional start sites (TSSs) (Moqtaderi et al., 2010; Oler et al., 2010), and expressed tRNA genes are predominantly located in the vicinity of active Pol II promoters (Oler et al., 2010). Thus, Pol III and Pol II transcription may be functionally linked.

Gene expression is regulated by multiple mechanisms, including the interaction of promoters with distal enhancers, which are short genomic elements (typically < 200 bp) often positioned several kilobases away from their target genes (Kolovos et al., 2012). Enhancers function in an orientation-independent manner and are characterized by distinctive features, such as an "open" chromatin and the presence of the histone modifications H3 lysine 4 monomethylation (H3K4me1) and lysine 27 acetylation (H3K27ac) (Heintzman et al., 2009; Kolovos et al., 2012; Zentner et al., 2011). Enhancers are often transcribed into non-coding RNAs known as enhancer RNAs (eRNAs), which stabilize the formation of DNA loops, possibly facilitating the interaction of enhancers with gene promoters (Kolovos et al., 2012). Recently, a distinct class of enhancers has been shown to provide spatiotemporal specificity to gene expression during neuronal development (Frank et al., 2015) and in mature neurons (Kim et al., 2010; Malik et al., 2014; Schaukowitch et al., 2014; Telese et al., 2015). However, the mechanisms by which they regulate transcription remain poorly understood.

We previously showed that, in neurons, a group of SINEs undergoes *de novo* histone acetylation and recruits the Pol III general transcription factor TFIIIC (Crepaldi et al., 2013). SINEs are an abundant class of retrotransposons often considered as non-functional DNA because of their non-coding, repetitive nature. They are short modular sequences that, similarly to other Pol III-transcribed genes, possess an internal Pol III promoter containing A and B boxes (Muotri et al., 2007; White, 2011). These elements bind the multi-subunit complex TFIIIC, which, in turn, recruits TFIIIB and Pol III. Most SINEs carry mutations that disrupt the promoter region, leaving only a few subtypes

This is an open access article under the CC BY license (http://creativecommons.org/licenses/by/4.0/).

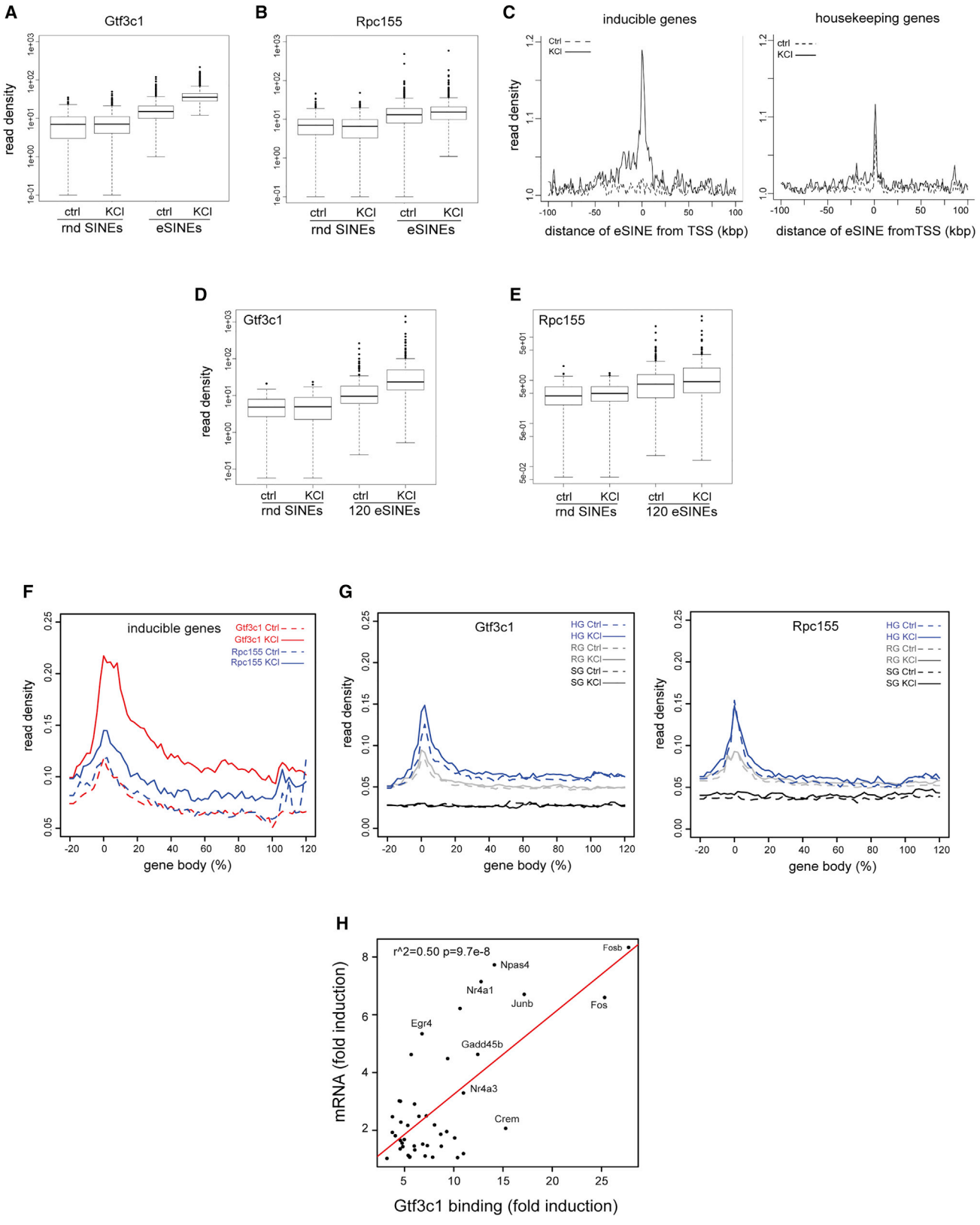

(legend on next page)

with transcriptional potential (Ichiyanagi, 2013). Recent studies indicated that SINEs often acquire novel functions in the host genome in a phenomenon known as exaptation (Huda et al., 2010; Rebollo et al., 2012). In mammalian fibroblasts exposed to heat shock, for example, SINE transcripts inhibited Pol II-dependent transcription by interacting with the Pol II enzyme (Allen et al., 2004; Mariner et al., 2008). Two members of the ancient SINE family Amniota SINE1 (AmnSINE1) were shown to act as enhancers for the *fibroblast growth factor 8* (*Fgf8*) and *special AT-rich sequence-binding protein 2* (*Satb2*) genes in the developing mouse brain (Sasaki et al., 2008; Tashiro et al., 2011). Similarly, in humans, members of the Alu family are enriched for enhancer-like histone modifications in a tissue-specific manner and preferentially engage in long-distance interactions with gene promoters and other Alu elements (Su et al., 2014).

Here, we identified a class of SINEs that function as enhancers of activity-regulated neuronal genes. Genome-wide analyses revealed that enhancer SINEs (eSINEs) bear the epigenetic marks H3K4me1 and H3K27ac, recruit TFIIIC, and are transcribed by Pol III in response to depolarization. We discovered that an eSINE located in the proximity of the activity-dependent gene *Fos* (which we named Fos^{RSINE1}) functions as a *Fos* enhancer and is transcribed in depolarized neurons. Fos^{RSINE1} eRNA interacts with Pol II at the *Fos* promoter and is necessary for the relocation of *Fos* to Pol II transcription factories upon depolarization. Strikingly, this mechanism is required for activity-dependent dendritogenesis and for cortical radial migration and neuronal differentiation of neural progenitors during embryonic development. Together, our findings demonstrate the profound effect of Fos^{RSINE1} on *Fos* gene expression and reveal a functional link between Pol III and Pol II transcription.

RESULTS

Genome-wide Occupancy of the Pol III Machinery Identifies eSINEs

In response to neuronal depolarization, a group of SINEs located near activity-dependent genes undergoes *de novo* acetylation at H3K9/K14 (Crepaldi et al., 2013). Because acetylated SINEs possess an internal Pol III promoter (Muotri et al., 2007; White, 2011), we reasoned that they may represent a class of Pol III-transcribed neuronal enhancers. To investigate this hypothesis, we first employed chromatin immunoprecipitation sequencing (ChIP-seq) to map the Pol III machinery genome-wide in resting or depolarized mouse primary cortical neurons. We employed paired-end sequencing to obtain reads that were significantly longer than SINEs and, therefore, easily mappable (Figure S1A). For each experimental condition, we produced over 32 million high-quality mapped reads, providing excellent depth (Figure S1B).

ChIP-seq was performed using antibodies that recognize the catalytic subunit of Pol III (Rpc155) or the DNA binding subunit of TFIIIC (Gtf3c1). As expected, both Rpc155 and Gtf3c1 were highly enriched at tRNA genes (Figures S1C and S1D). Gtf3c1 was widely distributed across the genome, with 66,662 and 58,090 peaks in control (Ctrl) and depolarized conditions, respectively (Table S1). Similar to other cell types (Barski et al., 2010; Oler et al., 2010), only a small fraction of Gtf3c1 binding sites recruited Rpc155 (14.8% and 6.1% in Ctrl and depolarized conditions, respectively; Table S1). Interestingly, a considerable fraction of Rpc155 and Gtf3c1 peaks overlapped at least one SINE (17.4% and 20.0% in resting and stimulated neurons, respectively, for Gtf3c1 and 20.7% and 21.1% for Rpc155; Table S1). Comparative analysis in untreated and depolarized neurons revealed that 7,700 genomic regions showed significant recruitment of Gtf3c1 in response to depolarization, of which 1,151 overlapped with SINEs (Table S2). We named this group of 1,151 SINEs characterized by activity-dependent recruitment of TFIIIC eSINEs. The levels of Gtf3c1 binding to these elements were higher than for randomly selected SINEs (rndSINEs, $p < 2.2e{-}16$, Mann-Whitney test for both Ctrl and KCl conditions; Figure 1A). Importantly, Gtf3c1 binding to eSINEs increased in response to stimulation ($p < 2.2e{-}16$, Mann-Whitney test), whereas it was unchanged for rndSINEs. Similarly, Pol III binding was higher on eSINEs compared with rndSINEs ($p < 2.2e{-}16$, Mann-Whitney test for both Ctrl and KCl conditions; Figure 1B), and recruitment to eSINEs increased in KCl-treated neurons ($p = 2.9e{-}11$, Mann-Whitney test). ChIP-seq tracks of representative eSINEs are shown in Figure S1E.

To investigate whether Gtf3c1 recruitment to eSINEs correlated with activity-dependent transcription genome-wide, we analyzed RNA sequencing (RNA-seq) data performed under similar experimental conditions (Kim et al., 2010; Malik et al., 2014). We observed that eSINEs were enriched in the proximity of inducible, but not housekeeping, genes (Figure 1C). Although

Figure 1. Genome-wide Identification of eSINEs

(A and B) Box and whisker plots of Gtf3c1 (A) and Rpc155 (B) distribution. Shown is ChIP-seq tag density at eSINEs or at randomly selected SINEs (rndSINEs) of comparable size. The solid line denotes the median. Lower and upper box limits indicate the 25th and 75th percentiles, respectively. Whiskers indicate 1.5 times the interquartile distance, measured from the median.

(C) Distribution of Gtf3c1-bound eSINEs under control (dashed line) or depolarized (solid line) conditions relative to the TSS of inducible (left) and housekeeping genes (right).

(D and E) Box and whisker plots summarizing the distribution of Gtf3c1 (D) and Rpc155 (E). Shown is ChIP-seq tag density at 120 eSINEs or at 120 randomly selected SINEs of comparable size. The solid line denotes the median. Lower and upper box limits indicate the 25th and 75th percentiles, respectively. Whiskers indicate 1.5 times the interquartile distance, measured from the median.

(F and G) Binding density profiles of Gtf3c1 and Rpc155 at gene bodies of the indicated sets of genes under control (dashed line) or depolarized (KCl, 50 mM for 45 min, solid line) neurons. Inducible genes (IGs, F), housekeeping genes (HGs, G), a randomly selected set of genes (RGs, G), and silent genes (SGs, G) were analyzed.

(H) Transcription of activity-regulated genes correlates with Gtf3c1 recruitment to proximal eSINEs. mRNA fold induction for each gene is plotted versus Gtf3c1 induction at the closest eSINE. R2 (Pearson correlation coefficient) and p value are shown.

See also Figure S1.

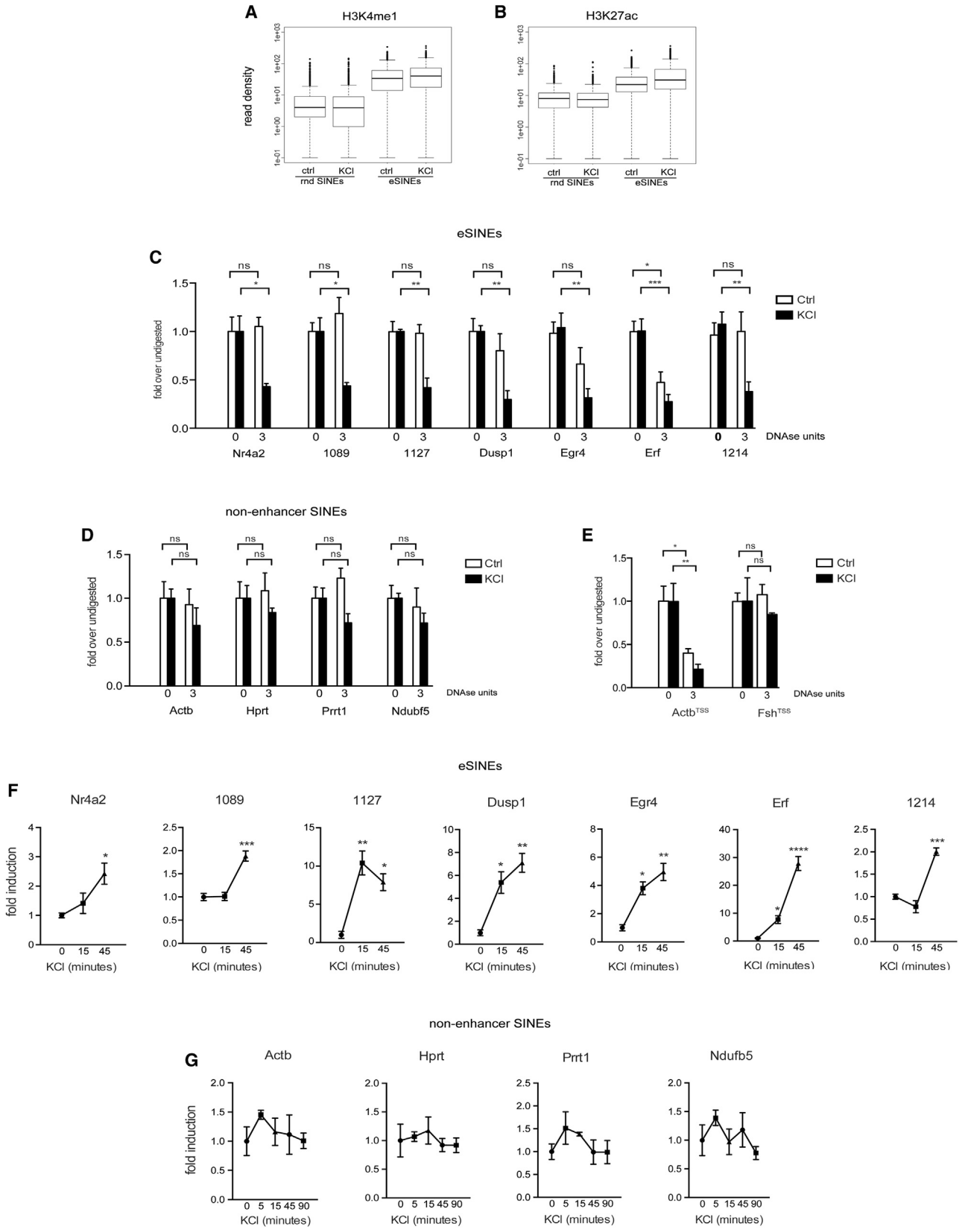

(legend on next page)

alternative roles cannot be excluded, this genomic localization suggests that eSINEs may represent a new class of regulatory elements that coordinate activity-dependent transcription in neurons. Next, 120 genes that were induced at least 2-fold in response to depolarization were paired with the closest eSINE (distances ranging from < 1 kb to several hundred kilobases from the TSS; Table S3). This group of eSINEs showed recruitment of the Pol III machinery in response to depolarization (Figures 1D and 1E, right plots; $p < 2.2e{-}16$ and $p = 2.1e{-}7$ for Gtf3c1 and Rpc155 respectively, Mann-Whitney test) whereas 120 rndSINEs did not (Figures 1D and 1E, left plots).

In accordance with previous studies indicating that Pol II and Pol III co-localize on the proximity of expressed genes, the enrichment of Rpc155 and Gtf3c1 at the TSSs and gene bodies of the paired 120 genes increased in depolarized neurons (Figure 1F; Moqtaderi et al., 2010; Oler et al., 2010; Raha et al., 2010). As expected, no significant recruitment of the Pol III machinery was observed on housekeeping genes (HGs; Figure 1G); lower occupancy of Pol III and Gtf3c1 was observed at randomly selected genes (RGs) and silent genes (SGs), with no changes upon neuronal activity (Figure 1G). A positive correlation ($r^2 = 0.5$, $p = 9.7e{-}8$; Figure 1H) was found between the recruitment of Gtf3c1 at eSINEs following depolarization and the transcription of genes for which the closest eSINE was located at a distance of 100 bp or less from the TSS (45 of 120 genes). This subset of genes included *Fos*, *Gadd45b*, and other well-characterized activity-dependent genes, such as *FosB*, *JunB*, *Egr4*, *Crem*, *Npas4*, *Nr4a1*, and *Nr4a3* (Figure 1H; Table S3).

eSINEs Bear the Epigenetic Hallmarks of Enhancers and Are Transcribed

Epigenetic marks commonly used to identify putative enhancers include H3K27ac and H3K4me1 (Kolovos et al., 2012; Zentner et al., 2011). ChIP-seq experiments performed on Ctrl and depolarized neurons revealed that both histone modifications were higher at the 1,151 eSINEs than at rndSINEs ($p < 2.2e{-}16$, Mann-Whitney test for both Ctrl and KCl conditions; Figures 2A and 2B). H3K4me1 and H3K27ac were present at eSINEs in resting neurons, indicating that they may be epigenetically primed prior to neuronal activation. H3K4me1 and H3K27ac were also enriched at the 120 eSINEs paired with activity-dependent genes ($p = 2.5e{-}15$ and $p = 6.2e{-}12$, respectively, under Ctrl conditions; Figures S2A and S2B). The recruitment of Gtf3c1 to a panel of eSINEs in response to depolarization and the presence of H3K4me1 and H3K27ac were confirmed using ChIP-qPCR (Figure S2C). It should be noted that eSINEs displayed levels of H3K4me1 and H3K27ac similar to previously identified enhancers for the activity-dependent genes *Arc* and *Fos* (Kim et al., 2010; Schaukowitch et al., 2014; Figure S2C). In contrast, SINEs located in the proximity of housekeeping (*Actb* and *Hprt*) and repressed (*Prrt1* and *Ndufb5*) genes did not recruit Gtf3c1 and were devoid of the enhancer marks H3K4me1 and H3K27ac (Figure S2C).

Enhancers are active genomic regions that, similarly to promoters, are associated with an open, easily accessible state of the chromatin (Boyle et al., 2008; Frank et al., 2015). When the chromatin accessibility of eSINEs was tested using the DNaseI hypersensitivity assay, we observed increased sensitivity to DNaseI digestion after depolarization (Figure 2C), indicating that the chromatin surrounding eSINEs becomes depleted of nucleosomes and primed for transcription. In contrast, SINEs located in the proximity of either housekeeping (*Actb* and *Hprt*) or repressed (*Prrt1* and *Ndufb5*) genes were not sensitive to DNaseI (Figure 2D). Notably, the hypersensitivity of eSINEs to DNaseI after neuronal stimulation was comparable with that observed at the TSS of the housekeeping gene *Actb* (*actin beta*; Figure 2E), whereas *Fsh* (*follicle-stimulating hormone*), a gene that is not expressed in neurons, did not show DNaseI hypersensitivity (Figure 2E).

Enhancers are transcribed in a number of organisms and cell types in response to external stimuli (Kaikkonen et al., 2013; Koch et al., 2011; Wang et al., 2011), and the eRNAs produced are critical for enhancer function (Lam et al., 2013; Li et al., 2013; Melo et al., 2013; Schaukowitch et al., 2014; Telese et al., 2015). We therefore investigated whether eSINEs were expressed in response to neuronal depolarization using qRT-PCR and found that they were transcribed in activated neurons (Figure 2F). Importantly, eSINE RNAs terminated in the proximity of canonical Pol III transcriptional terminators (Figure S3), indicating that they are *bona fide* Pol III transcripts. As expected, SINEs located proximal either to housekeeping (*Actb* and *Hprt*) or repressed (*Prrt1* and *Ndufb5*) genes were not transcribed (Figure 2G). Thus, eSINEs represent a new class of neuronal enhancers that recruit TFIIIC and are transcribed by Pol III.

Functional Characterization of Fos^{RSINE} and $Gadd45b^{B1F}$ eSINEs

To gain further insights into the biochemical and functional properties of eSINEs, two elements located in the proximity of *Fos* and *Gadd45b* (named Fos^{RSINE1} and $Gadd45b^{B1F}$) were selected for further analysis. *Fos* and *Gadd45b* are activity-dependent genes with well known functions in the nervous system (Greenberg et al., 1986; Ma et al., 2009) that are transcribed *in vivo* in cortical neurons upon exposure to a novel enriched

Figure 2. eSINEs Show the Hallmarks of Enhancers and Are Transcribed

(A and B) Box and whisker plots summarizing the distribution of H3K4me1 (A) and H3K27ac (B). Shown is ChIP-seq tag density at eSINEs or at randomly selected SINEs of comparable size. The solid line denotes the median. Lower and upper box limits indicate the 25th and 75th percentiles, respectively. Whiskers indicate 1.5 times the interquartile distance, measured from the median.

(C–E) Cortical neurons were treated with DNaseI (3 units for 20 min, 3) or vehicle (0) and depolarized with KCl for 45 min. Histograms show DNaseI digestion efficiency at eSINEs (C), non-enhancer SINEs (D), and the TSS of *Actb* and *Fsh* (E) expressed as fold over undigested. Data are represented as mean ± SEM (n = 3). *p < 0.05, **p < 0.01, ***p < 0.001, two-way ANOVA.

(F and G) Expression profile of a panel of eSINEs (F) and non-enhancer SINEs (G) in response to KCl stimulation, assessed by qRT-PCR. Data are represented as mean ± SEM and normalized to 0 min KCl (n = 3). *p < 0.05, **p < 0.01, ***p < 0.001, ****p < 0.0001, one-way ANOVA.

See also Figures S2 and S3.

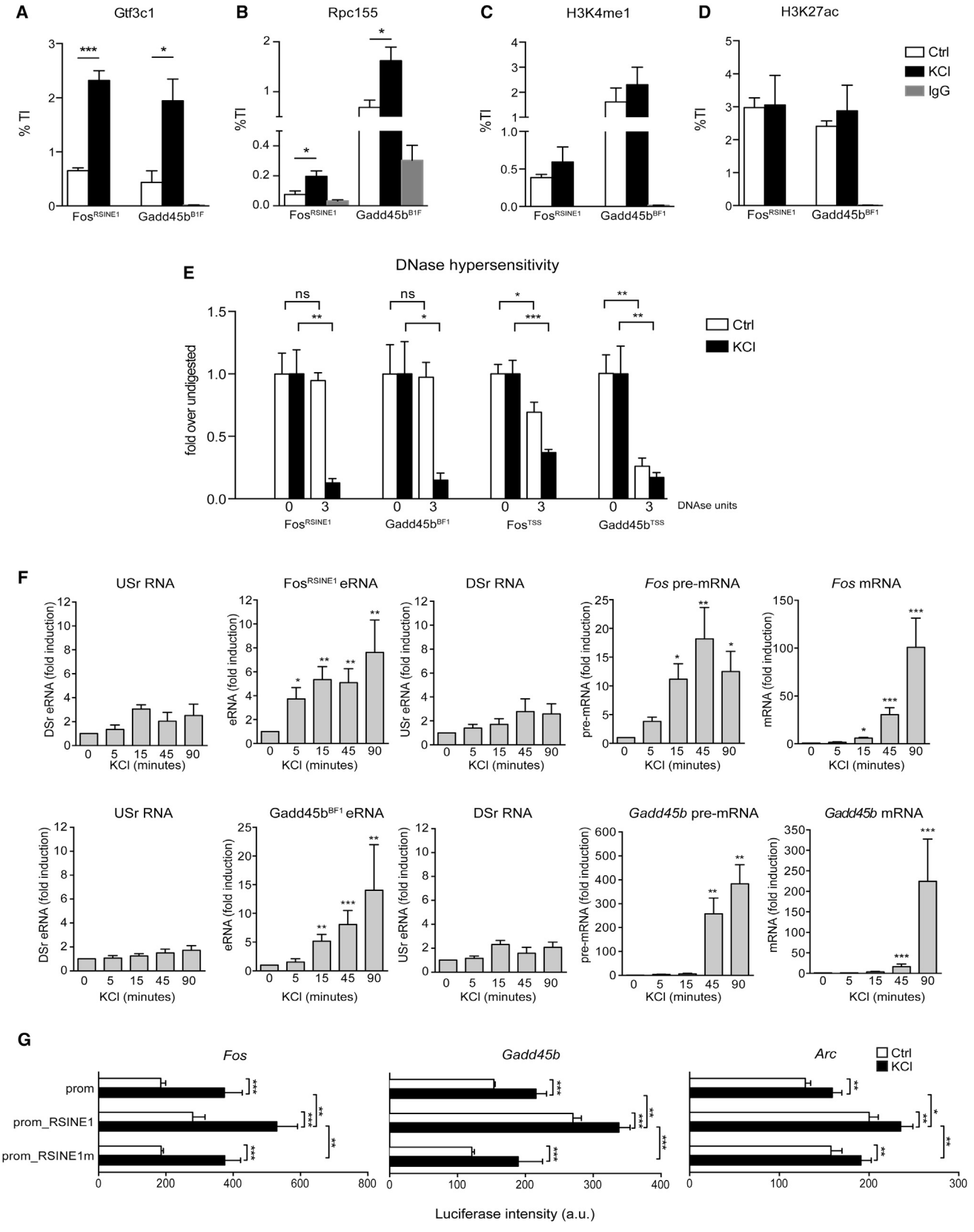

(legend on next page)

environment (NEE) and in response to neuronal depolarization *in vitro* (Crepaldi et al., 2013; Sheng et al., 1990; Sultan et al., 2012). Moreover, both eSINEs are *de novo* acetylated on H3K9K14 in the somatosensory cortex of mice exposed to NEE (Crepaldi et al., 2013). Despite the fact that SINE sequences are highly repetitive, Fos^{RSINE1} and Gadd45b^{B1F} have distinctive features that allow unequivocal identification (Figure S4A). We first confirmed that Fos^{RSINE1} and Gadd45b^{B1F} recruited Gtf3c1 and Rpc155 in response to depolarization (Figures 3A and 3B) and displayed the H3K4me1 and H3K27ac marks (Figures 3C and 3D). Fos^{RSINE1} and Gadd45b^{B1F} also showed activity-dependent hypersensitivity to DNaseI comparable to *Fos* and *Gadd45b* TSSs (Figure 3E). qRT-PCR of Fos^{RSINE1} and Gadd45b^{B1F} RNA at different times after neuronal depolarization revealed that both eSINEs are robustly transcribed (Figure 3F). Importantly, transcription was not detected at genomic regions located immediately upstream (USr) or downstream (DSr) of Fos^{RSINE1} (−170 and +750 bp) and Gadd45b^{B1F} (−400 and +200 bp) (Figure 3F), indicating that the eSINEs are not part of larger transcriptional units. Interestingly, expression of both Fos^{RSINE1} and Gadd45b^{B1F} preceded *Fos* and *Gadd45b* transcription (Figure 3F), suggesting that Fos^{RSINE1} and Gadd45b^{B1F} eRNA may control the expression of these genes.

We next investigated whether Fos^{RSINE1} enhanced activity-dependent transcription using luciferase reporter assays. Neurons were transfected with plasmids expressing the luciferase coding region under the control of three activity-response gene promoters (*Fos*, *Gadd45b*, and *Arc*) and either depolarized or left untreated. Under stimulated conditions, inclusion of Fos^{RSINE1} at the 3′ end of the luciferase cassette markedly increased luciferase expression for all tested promoters (Figure 3G). Fos^{RSINE1} did not enhance luciferase expression when cloned 3′ of either the SV40 promoter of the pGL3-promoter vector or the *Gapdh* promoter (Figures S4B and S4C). Importantly, in neurons transfected with equimolar amounts of a vector carrying Fos^{RSINE1} and a separate luciferase construct encoding the *Fos* promoter, Fos^{RSINE1} failed to enhance luciferase expression (Figure S4D), indicating that genomic contiguity is required for enhancer function.

To establish whether transcription of Fos^{RSINE1} is necessary for enhancer function, we generated a mutated version of the eSINE bearing a six-nucleotide mismatch that disrupts Gtf3c1 and Pol III recruitment (Orioli et al., 2012). Mouse neuroblastoma cells (Neuro-2a) were transfected with a vector carrying either wild-type (pBS_RSINE1WT) or mutant Fos^{RSINE1} (pBS_RSINE1mut) and stimulated with forskolin. Fos^{RSINE1} expression levels were significantly lower in cells transfected with the mutant compared with the wild-type vector (Figure S4E). Strikingly, this mutated version of Fos^{RSINE1} failed to enhance activity driven by *Fos*, *Gadd45b*, and *Arc* promoters (Figure 3G). Thus, Pol III binding to Fos^{RSINE1} is required for enhancer activity.

Fos^{RSINE} eRNA Is Required for Enhancer Function

To investigate the mechanisms by which eSINEs regulate activity-dependent transcription, the Fos^{RSINE1} genomic sequence was disrupted using a high-fidelity variant of Cas9 (SpCas9-HF1; Kleinstiver et al., 2016). A guide RNA targeting Fos^{RSINE1} was expressed in Neuro-2a cells together with a vector encoding SpCas9-HF1. As a control, we transfected the SpCas9-HF1-encoding plasmid and an empty vector (no guide). Efficient editing of the Fos^{RSINE1} locus was assessed by Surveyor assay (Figure S5A) and confirmed by DNA sequencing of individual clones (Figure S5B). In cells transfected with Fos^{RSINE1} guide RNA, the induction of Fos^{RSINE1} eRNA upon forskolin stimulation was drastically reduced compared with empty vector (Figure 4A), whereas induction of a different eSINE (Dusp1^{MIRc}) was not affected by (Figure 4A). Strikingly, disruption of the Fos^{RSINE1} genomic locus was sufficient to abolish forskolin-dependent transcription of *Fos* (Figure 4A), indicating that the genomic integrity of Fos^{RSINE1} is necessary for *Fos* expression upon neuronal stimulation.

Experiments that knockdown eRNAs have recently shown that enhancer transcripts regulate the expression of nearby genes (Lam et al., 2013; Li et al., 2013; Melo et al., 2013; Mousavi et al., 2013; Schaukowitch et al., 2014). To investigate whether Fos^{RSINE1} enhancer activity is mediated by Pol III-dependent eRNA synthesis, we employed several complementary approaches. First, cortical neurons were treated with the specific Pol III inhibitor ML60218 (50 μM, 15 min; Wu et al., 2003) and depolarized. ML60218 treatment decreased transcription of the Pol III-transcribed gene *tRNALeu* (Figure S6A), indicating efficient inhibition of Pol III. Importantly, inhibition of Pol III markedly reduced transcription of both Fos^{RSINE1} and the *Fos* gene in response to neuronal activation (Figures 4B and 4C). The effect of ML60218 on *Fos* transcription was not due to non-specific inhibition of Pol II because the expression levels of the Pol II-transcribed *β-Actin* were unchanged (Figure S6B). Conversely, treatment of cortical neurons with the specific Pol II inhibitor 5,6-dichloro-1-β-D-ribofuranosylbenzimidazole (DRB) (Yankulov et al., 1995) led to a strong reduction in *Fos* induction and *β-Actin* transcription but had no effect on either Fos^{RSINE1} or *tRNALeu* transcription (Figures 4B and 4C; Figures S6A and

Figure 3. Fos^{RSINE1} and Gadd45b^{B1F} Are *Bona Fide* eSINEs

(A–D) Mouse cortical neurons were exposed to KCl (50 mM, 45 min) or left untreated and subjected to Gtf3c1 (A), Rpc155 (B), H3K4me1 (C), and H3K27ac (D) ChIP-qPCR. Histograms show ChIP efficiency expressed as percentage of chromatin input; immunoglobulin G (IgG) ChIP was used as a negative control. Data are represented as mean ± SEM (n = 3). *p < 0.05, ***p < 0.001, Student's t test.

(E) Cortical neurons were treated with DNaseI (3 units for 20 min, 3) or vehicle (0) and depolarized with KCl. Histograms show DNaseI digestion efficiency expressed as fold over undigested. Data are represented as mean ± SEM (n = 3). *p < 0.05, **p < 0.01, ***p < 0.001, two-way ANOVA.

(F) KCl-dependent expression levels of Fos^{RSINE1}, Gadd45b^{B1F}, *Fos*, *Gadd45b*, and the genomic regions located immediately upstream (USr) or downstream (DSr) of the two SINEs were analyzed by qRT-PCR. *Fos* (top) and *Gadd45b* (bottom). Data are represented as mean ± SEM (n ≥ 5). *p < 0.05, **p < 0.01, ***p < 0.001, one-way ANOVA.

(G) Luciferase assay of mouse cortical neurons transfected with the indicated vectors and stimulated with KCl for 6 hr or left untreated. Data are represented as mean ± SEM (n ≥ 3). *p < 0.05, **p < 0.01, ***p < 0.001, two-way ANOVA.

See also Figure S4.

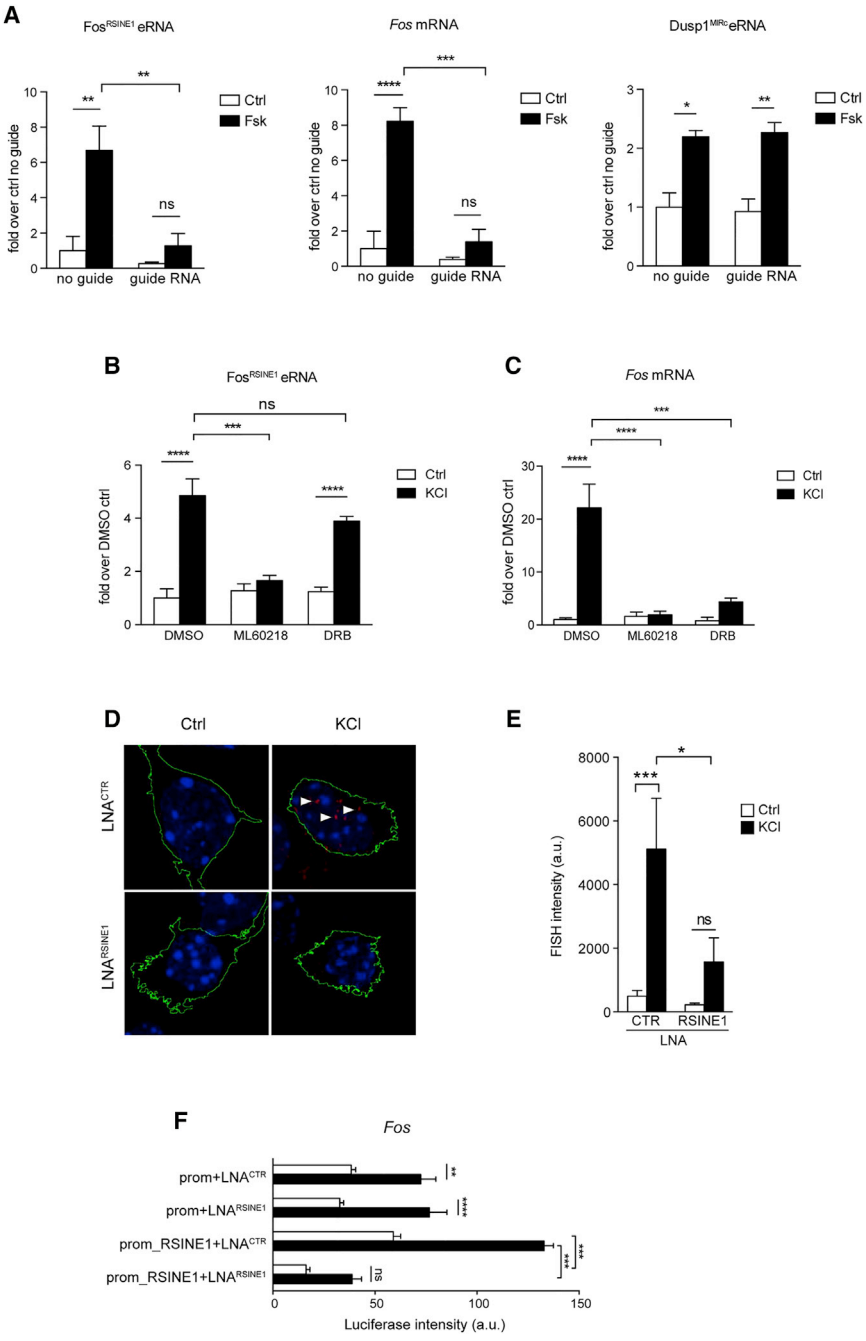

Figure 4. Fos^{RSINE1} eRNAs Is Required for Enhancer Functions

(A) Neuro-2a cells were transfected with a vector encoding SpCas9-HF1 protein and either an empty RNA vector (BPK1520, no guide) or an RNA vector containing a small guide RNA targeting Fos^{RSINE1} (guide RNA). Cells were either left untreated or treated with forskolin (50 μM, 45 min). Shown are mean ± SEM of fold induction of Fos^{RSINE1}, Fos, and Dusp1MIRc over control no guide (n = 4). *p < 0.05, **p < 0.01, ***p < 0.001, ****p < 0.0001, two-way ANOVA.

(B and C) qRT-PCR of cortical neurons treated with ML60218 (50 μM, 15 min) or DRB (25 μM, 15 min) and exposed to KCl for 45 min. Shown are mean ± SEM of fold induction over DMSO control of Fos^{RSINE1} eRNA (B) and *Fos* mRNA (C) (n = 3). *p < 0.05, **p < 0.01, two-way ANOVA.

(D) RNA FISH analysis of *Fos* mRNA in cortical neurons transfected with GFP and either LNA^{CTR} or LNA^{RSINE1} and exposed to KCl for 45 min or left untreated. Shown are maximal projections of confocal scans; reconstructed cell edges are shown in green, DAPI-counterstained nuclei are shown in blue, and Fos mRNA ribonucleoparticles are shown in red.

(E) Quantitative analysis of RNA FISH experiments. Shown are means ± SEM of at least 42 cells per condition (n = 3). *p < 0.05, ***p < 0.001, two-way ANOVA.

(F) Luciferase assay of cortical neurons transfected with the indicated vectors in combination with either LNA^{CTR} or LNA^{RSINE1}. Data shown as mean ± SEM (n = 4). **p < 0.01, ***p < 0.001, ****p < 0.0001, two-way ANOVA.

See also Figures S5–S7.

S6B). Similar results were obtained for two additional eSINEs (Gadd45b^{B1F} and Dusp1^{MIRc}) and the paired activity-dependent genes (*Gadd45b* and *Dusp1*) (Figures S6C–S6F).

Next we used locked nucleic acid (LNA) oligonucleotides to specifically target Fos^{RSINE1} eRNA for degradation. In Neuro-2a cells, an LNA targeting Fos^{RSINE1} eRNA (LNA^{RSINE1}) reduced Fos^{RSINE1} levels without affecting Dusp1^{MIRc} expression (Figures S6G and S6H). Cortical neurons were transfected with either LNA^{RSINE1} or a control LNA (LNA^{CTR}) and depolarized, and the *Fos* transcript was measured using RNA fluorescence *in situ* hybridization (FISH). As expected, in LNA^{CTR}-treated neurons depolarization induced the appearance of clearly detectable ribonucleoparticles containing *Fos* mRNA (Figure 4D, top right, white arrowheads). Remarkably, LNA^{RSINE1} caused a 70% reduction of *Fos* mRNA expression compared with LNA^{CTR} (Figures 4D and 4E). Similarly, an LNA targeting Dusp1^{MIRc} eRNA (LNA^{MIRc}) strongly reduced *Dusp1* mRNA levels following KCl stimulation (Figures S7A and S7B). The specificity of LNA^{RSINE1} was tested by performing luciferase assays on neurons expressing vectors encoding luciferase under the control of either the *Fos* promoter and Fos^{RSINE1} (prom_RSINE1) or the *Fos* promoter alone (prom). In neurons transfected with prom_RSINE1, LNA^{RSINE1} completely abolished Fos^{RSINE1} enhancer activity but was ineffective in decreasing luciferase expression in neurons transfected with a vector containing *Fos* promoter only (Figure 4F). Together, these data show that Pol III-dependent transcription of Fos^{RSINE1} is necessary for enhancing *Fos* expression in depolarized neurons.

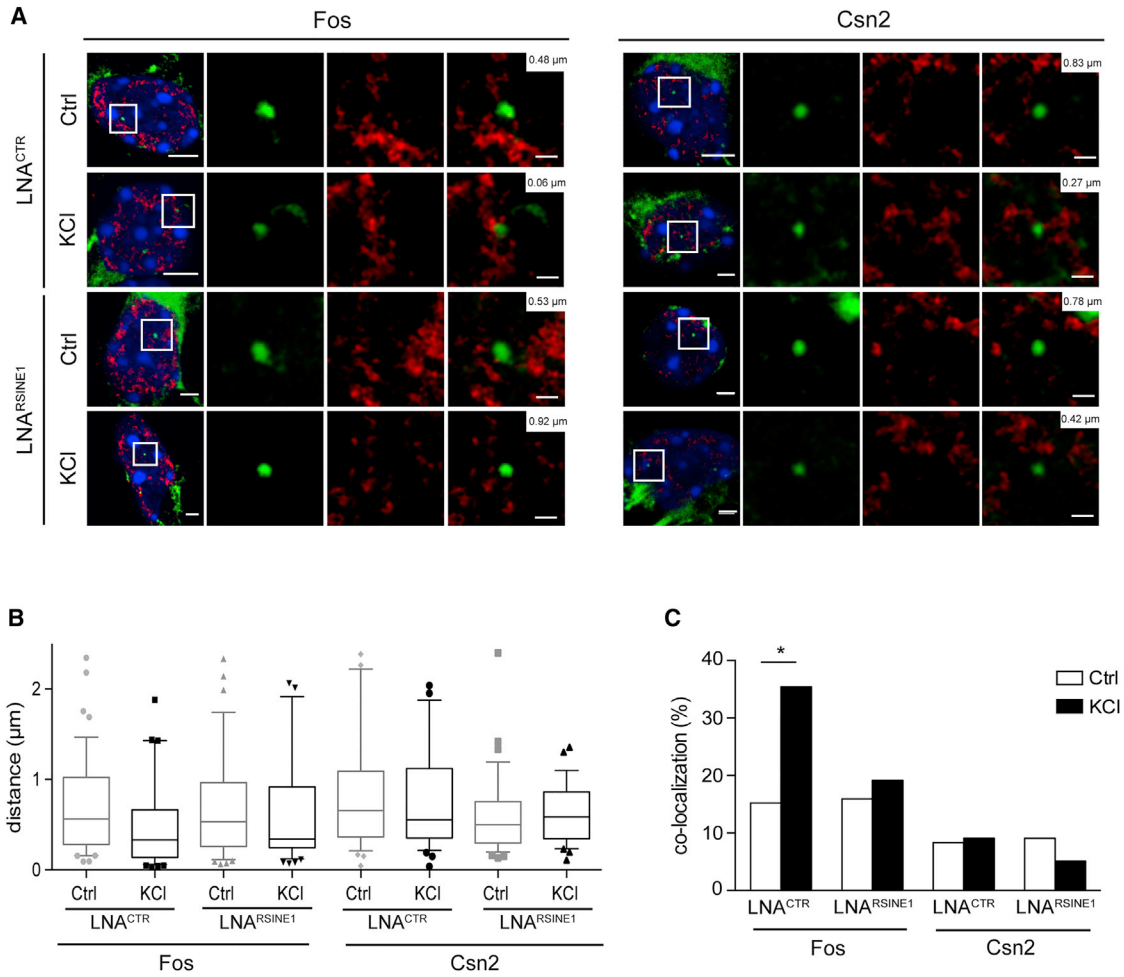

Figure 5. Fos^{RSINE1} eRNA Mediates *Fos* Relocation to Transcription Factories

(A) Representative images of confocal sections of immuno-DNA FISH showing nuclear localization of *Fos* and *Csn2* loci (green) relative to TFs in neurons transfected with GFP and either LNA^{CTR} or LNA^{RSINE1} and exposed to KCl for 45 min or left untreated. TFs were detected by Pol II immunostaining (4H8, red); nuclei were stained with DAPI (blue). For each image series, the distance between the center of the FISH signal and the nearest TF is indicated (top right inset). Scale bars, 2 μm (images on the left) and 0.5 μm (magnified images).

(B) Box and whisker plot of the distribution of the distance between *Fos* or *Csn2* loci and the nearest TF. Whiskers denote the 90th and 10th percentiles, box edges denote the 75th and 25th percentiles, solid lines denote medians, and dashed lines denote averages. n = 33–48 foci across 3 biological replicates.

(C) Percentage of co-localization of the *Fos* and *Csn2* loci with TFs, both under basal conditions and in response to KCl, in neurons transfected with either LNA^{CTR} or LNA^{RSINE1}. *p < 0.05, Fisher's exact test.

Fos^{RSINE1} eRNA Controls *Fos* Gene Relocation to Transcription Factories

Transcription factories (TFs) are discrete nuclear foci formed by clusters of Pol II and transcription factors that create a permissive environment for transcription (Rieder et al., 2012) where enhancers and promoters may physically interact (Cook, 2010). Because activity-dependent genes relocate to TFs upon depolarization (Crepaldi et al., 2013), we investigated whether eSINE eRNA regulates this process by performing immuno-DNA FISH on cortical neurons transfected with LNAs (Figure 5A). TFs were labeled using a Pol II antibody, and the distance between the center of the DNA-FISH signal and the nearest TF was measured. In neurons transfected with LNA^{CTR}, neuronal stimulation decreased the distance between the *Fos* locus and the nearest TF (Figure 5B) and led to higher co-localization of FISH signals with TFs (Figure 5C). Strikingly, transfection with LNA^{RSINE1} inhibited depolarization-dependent relocation of *Fos* to TFs (Figures 5A–5C), whereas the nuclear position of *Csn2*, a gene that is not expressed in neurons, was not affected (Figures 5A–5C). Our findings indicate that Fos^{RSINE1} eRNA promotes *Fos* relocation to TFs in response to stimulation and may contribute to the spatial organization of chromatin within neuronal nuclei.

Fos^{RSINE1} eRNA Interacts with Pol II to Mediate Transcriptional Initiation and Elongation

It has been proposed that eRNAs may contribute to Pol II loading onto target promoters (Mousavi et al., 2013). Moreover,

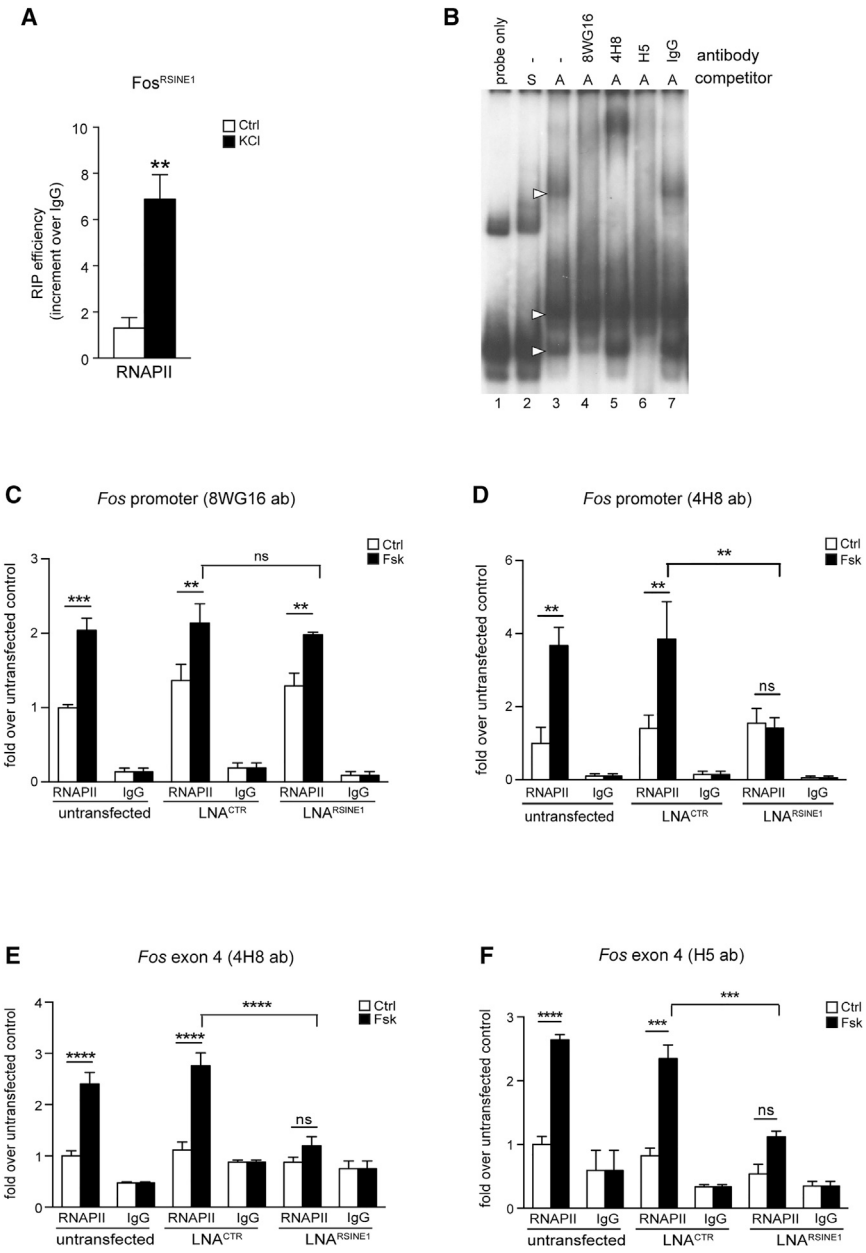

Figure 6. Fos^{RSINE1} eRNA Interacts with Pol II and Affects Pol II Initiation and Elongation

(A) RNA immunoprecipitation (RIP) of cortical neuron nuclear extracts incubated with Pol II 8WG16 antibody and subjected to qRT-PCR. RIP efficiency was expressed as increment over control IgG. Data are represented as mean ± SEM (n = 3). **p < 0.005, Student's t test.

(B) EMSA of Fos^{RSINE1} eRNA. A Fos^{RSINE1} radiolabeled probe was incubated with cortical neuron nuclear extracts. An excess of either sense (S) or antisense (A) unlabeled probe was used as control. Three bands were detected (lane 3, white arrowheads) that were super-shifted or displaced by Pol II antibodies (lanes 4–6).

(C–F) Neuro-2a cells were transfected with the indicated LNAs, stimulated with forskolin (Fsk), and subjected to ChIP using 8WG16 (C), 4H8 (D and E), and H5 (F) antibodies. Histograms show ChIP efficiency at the *Fos* promoter and exon 4, expressed as fold over control. Data are shown as mean ± SEM (n = 3). **p < 0.01, ***p < 0.001, ****p < 0.0001, two-way ANOVA.

transcripts originating from SINEs have been shown to bind Pol II in mouse fibroblasts (Allen et al., 2004; Mariner et al., 2008). To investigate whether Fos^{RSINE1} eRNA interacted with Pol II, neurons were subjected to RNA immunoprecipitation (RIP) using a Pol II antibody. We observed that, upon depolarization, the Pol II antibody immunoprecipitated Fos^{RSINE1} eRNA at high levels (Figure 6A), indicating binding. Additional evidence of the interaction was obtained by performing electrophoretic mobility shift assays (EMSAs) using *in vitro*-transcribed α-^{32}P-labeled Fos^{RSINE1} eRNA. The radioactive probe was loaded on a nondenaturing polyacrylamide gel either alone (probe only) or in the presence of neuronal nuclear proteins. At least three distinct protein complexes were bound to Fos^{RSINE1} eRNA (Figure 6B, lane 3, white arrowheads). Antibodies that recognize the pre-initiating, initiating, or elongating forms of Pol II (8WG16, 4H8, and H5, respectively; Sutherland and Bickmore, 2009) displaced or super-shifted at least one band, confirming that Fos^{RSINE1} eRNA was associated with Pol II and indicating that the interaction can occur at different stages of transcription (Figure 6B, lanes 4–6).

We next asked whether Fos^{RSINE1} eRNA influenced Pol II recruitment to the endogenous *Fos* promoter using Pol II ChIP. In untransfected or LNA^{CTR}-transfected Neuro-2a cells, Pol II binding to the *Fos* gene significantly increased upon stimulation at both the promoter (8WG16 and 4H8 antibodies) and at the coding region (4H8 and H5 antibodies) (Figures 6C–6F). In cells transfected with LNA^{RSINE1}, stimulus-dependent binding of pre-initiating Pol II to the *Fos* promoter was conserved (Figure 6C), whereas recruitment of both the initiating and elongating forms of Pol II at the *Fos* promoter and coding region was prevented (Figures 6D–6F). These results indicate that, in the absence of the Fos ^{RSINE1} eRNA, Pol II is unable to progress into active transcription and provide the first evidence of a functional link between a Pol III-dependent transcript and Pol II.

Fos^{RSINE1} eRNA Regulates Neuronal Differentiation and Cortical Development

The biological significance of Fos^{RSINE1}-dependent regulation of *Fos* transcription was investigated by studying dendritogenesis of primary cortical neurons. Dendritic growth in response to external cues requires the transcription of activity-regulated

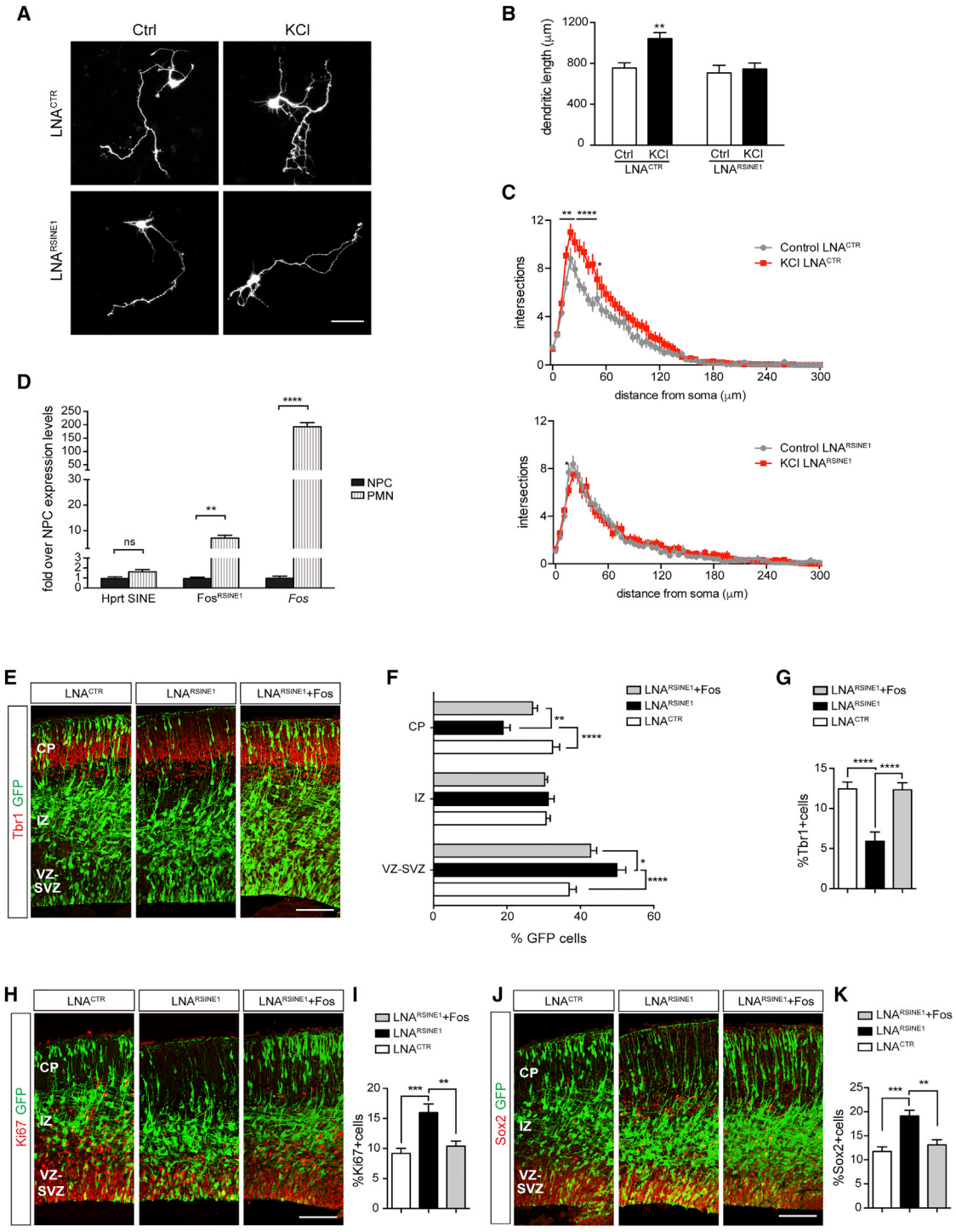

Figure 7. Fos^{RSINE1} Enhances *Fos* Expression in Diverse Physiological Contexts

(A) Representative images of cortical neurons transfected with a GFP-expressing vector in combination with either LNA^{CTR} or LNA^{RSINE1} and maintained under basal or depolarizing (KCl, 50 mM) conditions for 48 hr, followed by GFP immunostaining. Scale bar, 50 μm.

(B) Quantification of the total length of the dendritic processes of 29–31 neurons (n = 3). Shown are means ± SEM. **p < 0.01, two-way ANOVA.

(C) Sholl analysis of neurons analyzed in (B). For each distance point, the average number of intersections ± SEM is shown. *p < 0.05, **p < 0.01, ****p < 0.0001, two-way ANOVA.

(D) qRT-PCR of mouse neural progenitor cells (NPCs) and post mitotic-neurons (PMNs). Data show mean ± SEM of fold induction of Hprt SINE RNA, Fos^{RSINE1} eRNA, and Fos mRNA (n = 6) normalized to expression levels in NPCs. **p < 0.005, ****p < 0.0001, paired t test.

(legend continued on next page)

genes (West and Greenberg, 2011), many of which are regulated by Fos (Greenberg et al., 1986; Malik et al., 2014). Thus, early and robust activation of *Fos* may be necessary for dendritic arborization. Neurons were transfected with a GFP-expressing vector and either LNA^{CTR} or LNA^{RSINE1} and maintained under basal or depolarized conditions for 48 hr. As expected, neurons transfected with LNA^{CTR} showed an increase in both dendritic length and complexity (Figures 7A–7C). Strikingly, activity-dependent dendritogenesis was completely abrogated in neurons transfected with LNA^{RSINE1} (Figures 7A–7C).

Because *Fos* has been shown to regulate mouse brain development (Velazquez et al., 2015), we reasoned that Fos^{RSINE1} may also enhance *Fos* expression in this physiological context. First, we assessed whether Fos^{RSINE1} was expressed in embryonic cortical neurons. Mouse neural progenitor cells (NPCs) were dissected at embryonic day 12.5 (E12.5) and differentiated *in vitro* into post-mitotic neurons (PMNs) (Nitarska et al., 2016). A remarkable increase in both Fos^{RSINE1} and *Fos* expression levels was observed following differentiation of NPCs to PMNs (Figure 7D). Conversely, transcription of the non-enhancer SINE $Hprt^{SINE}$ was unchanged (Figure 7D). Next, we asked whether Fos^{RSINE1} regulated the expression of *Fos* during neuronal development *in vivo* by performing *in utero* electroporation experiments. LNA^{CTR} or LNA^{RSINE1} were electroporated together with a GFP expression plasmid into E13.5 mouse brains, and, after 2 days, neural migration and expression of differentiation markers were assessed. As observed previously (Nitarska et al., 2016) after 48 hr, 33% of the progeny of neural progenitors electroporated with LNA^{CTR} in the ventricular zone (VZ) had reached the cortical plate (CP) (Figures 7E and 7F). Inhibition of Fos^{RSINE1} expression resulted in an accumulation of cells within the VZ and a reduction of neurons migrating toward the CP (Figures 7E and 7F). Neural progenitors electroporated with LNA^{RSINE1} failed to differentiate and express T-Box Brain 1 (Tbr1) (Figures 7E and 7G), a transcription factor found in early-born neurons (Hevner et al., 2001). Consistent with the phenotype observed in $Fos^{-/-}$ mice (Velazquez et al., 2015), depletion of Fos^{RSINE1} eRNA also resulted in increased proliferation of neural progenitors, as indicated by the elevated number of Ki67- and Sox2-positive cells (Figures 7H–7K). Co-electroporation of neuronal progenitors with a vector expressing *Fos* under the control of a cytomegalovirus (CMV) early enhancer/chicken β-actin (CAG) promoter fully rescued the defects induced by the inhibition of Fos^{RSINE1} (Figures 7E–7K), ruling out potential off-target effects of LNA^{RSINE1}.

Thus, during the early stages of cortical development, Fos^{RSINE1} regulates radial migration and neuronal differentiation of NPCs, whereas at the onset of neuronal maturation, Fos^{RSINE1} eRNA is required for activity-dependent dendritogenesis.

DISCUSSION

eSINEs Are a Class of Neuronal Enhancers

Repetitive elements are extremely abundant in the mammalian genome, however their function remains largely obscure. In recent years, SINE transcripts have been linked to protein synthesis, mRNA turnover, and RNA editing in both human and mouse cell lines (Athanasiadis et al., 2004; Kim et al., 2004; Levanon et al., 2004; Ohnishi et al., 2012). SINEs may also have regulatory functions independent of their transcription, providing for example, sites of alternative splicing (Levanon et al., 2004), generating new TSSs and polyadenylation signals (Chen et al., 2009; Faulkner et al., 2009), and offering an accessible chromatin environment for transcription factor binding (Gomez et al., 2016). SINEs also act as insulators, transcriptional repressors, or developmentally regulated enhancers (Allen et al., 2004; Lunyak et al., 2007; Nakanishi et al., 2012; Tashiro et al., 2011). We have identified a new class of enhancer SINEs that are transcribed by Pol III and likely regulate the expression of many Pol II-dependent genes in response to neuronal depolarization. eSINEs share biochemical and functional properties with previously identified neuronal enhancers, including the epigenetic marks H3K4me1 and H3K27ac (Figures 2A and 2B, and 3C and 3D) and hypersensitivity to DNaseI (Figures 2C and 3E), which is associated with open, nucleosome-depleted chromatin. Importantly, although we were not able to perform a genome-wide analysis of eSINE transcripts because of technical issues related to their repetitive nature, we showed that many eSINEs are transcribed in response to neuronal depolarization (Figures 2F and 3F) and that transcription is critical for target gene induction (Figure 4; Figure S7).

A Functional Link between Pol III and Pol II Transcription

The Pol II and Pol III transcriptional machineries have been traditionally considered independent entities that regulate the expression of largely non-overlapping genes. However, recent studies have demonstrated that they often co-localize on genomic loci in both murine and human cells and that co-localization of the two machineries correlates with transcription (Barski et al., 2010; Moqtaderi et al., 2010; Oler et al., 2010; Raha et al., 2010). Whether the two machineries are functionally linked and the mechanisms of such regulation is still unknown.

Transcription of enhancer elements was first observed more than 20 years ago (Collis et al., 1990), and, more recently, RNA

(E) E13.5 embryos electroporated *in utero* with LNAs and a CAG-Fos-expressing construct as indicated and analyzed at E15.5. Shown are representative images of coronal sections immunolabeled for GFP (green) and Tbr1 (red). Scale bar, 100 μm.
(F) Quantification of the distribution of cells electroporated as in (E) between the ventricular-subventricular zone (VZ-SVZ), intermediate zone (IZ), and cortical plate (CP). Data are from 3 independent experiments and 16–22 embryos per condition.
(G) Quantification of neurons expressing Tbr1. Data are from 3 independent experiments and 16–22 embryos per condition.
(H) Coronal sections of mouse embryonic brains immunolabeled with GFP (green) and Ki67 (red) antibodies. Scale bar, 100 μm.
(I) Quantification of cells expressing Ki67. Data are from 3 independent experiments and 10–21 embryos per condition.
(J) Coronal sections of mouse brains immunolabeled with GFP (green) or Sox2 (red) antibodies. Scale bar, 100 μm.
(K) Histograms showing quantification of the percentage of cells expressing Sox2. Data are from 3 independent experiments and 10–21 embryos per condition. Data are represented as mean ± SEM; *p < 0.05, **p < 0.01, ***p < 0.001, ****p < 0.0001, two-way ANOVA with Tukey's post test (F) and one-way ANOVA with Tukey's post test (G, I, and K).

synthesis has been demonstrated at active enhancers of most cell types across many species (Kaikkonen et al., 2013; Koch et al., 2011; Wang et al., 2011). All neuronal enhancers identified to date are transcribed by Pol II and bind transcription factors that are also enriched on the promoter of their target genes (Kim et al., 2010; Malik et al., 2014; Telese et al., 2015). It has been postulated that recruitment of transcription factors to both enhancers and promoters helps to create a molecular bridge that physically connects the two elements, conferring specificity to enhancer-promoter pairings (Lam et al., 2014). In contrast, eSINEs are transcribed by Pol III and bind the general transcription factor complex TFIIIC (Figures 1A and 1B and 3A and 3B). Interestingly, eSINEs do not possess consensus sequences for any transcription factor associated with Pol II-transcribed neuronal enhancers (L.C. and A.R., unpublished data). Because TFIIIC and Pol III are recruited to both eSINEs and TSSs of activity-regulated genes (Figures 1A, 1B, and 1F), they may play a role in pairing eSINEs with their gene promoters in response to depolarization.

Binding of the Pol III machinery to eSINEs correlates with transcription of the closest genes in response to neuronal activation (Figure 1H), suggesting that contiguity of eSINEs with their target genes is necessary for enhancer functions. Consistent with this finding, Fos^{RSINE1} eRNA failed to enhance luciferase expression driven by the minimal *Fos* promoter when encoded by a separate vector (Figure S4D). However, the higher-order structure of chromatin within the nucleus enables enhancers to contact promoters even when they are located far apart on the chromosome. We discovered that Fos^{RSINE1} eRNA binds Pol II (Figures 6A and 6B) and is necessary for relocation of the *Fos* genomic region to transcription factories (Figure 5), perhaps inducing changes of chromatin structure that favor enhancer-promoter interactions. The finding that both Pol III and TFIIIC are recruited to Pol II-regulated genes (Figure 1F) further indicates that the two machineries may come into close proximity within transcription factories.

Fos^{RSINE1} Enhances *Fos* Expression in Diverse Physiological Contexts

The biological relevance of Fos^{RSINE1} was demonstrated by the fact that Fos^{RSINE1} eRNA is required for activity-dependent dendritic growth and branching (Figures 7A–7C). We previously showed that silencing of TFIIIC in cortical neurons increased dendritic length (Crepaldi et al., 2013). These findings may be explained by the fact that more than 80% of Gtf3c1 binding identified by ChIP-seq is located in genomic regions other than eSINEs and independently of Pol III (< 20% of co-localization on SINEs and < 15% genome-wide). Therefore, global silencing of TFIIIC is likely to affect genome organization and transcription in ways distinct from the inhibition of Fos^{RSINE1} and *Fos* expression alone. Strikingly, the role of Fos^{RSINE1} was not limited to regulating *Fos* expression in response to neuronal activity but extended to early brain development. Both *Fos* and Fos^{RSINE1} levels increased during neuronal differentiation *in vitro* (Figure 7D), and Fos^{RSINE1} eRNA was required for embryonic cortical development *in vivo* (Figures 7E–7K). Thus, in very different physiological contexts, Pol II-dependent transcription of the *Fos* gene is regulated by the Pol III-mediated transcription of its nearby eSINE.

In 1969 Britten and Davidson, formulated the hypothesis that transposable elements such as SINEs participate in gene-regulatory networks, contributing to speciation novelty (Britten and Davidson, 1969). More recently, repetitive elements have been shown to represent key determinants of macroevolution and clade-specific phenotypes (Tashiro et al., 2011). The considerable number of eSINEs identified in neurons suggests that they may have an unexpected and complex role that goes beyond controlling the expression of isolated genes and extend to globally linking Pol III with Pol II transcription.

EXPERIMENTAL PROCEDURES

CRISPR-Cas9

Single guide RNAs were designed toward the *Fos* eSINE using http://crispr.mit.edu/. The backbones for the vectors expressing the guide RNA (U6-BsmBIcassette-Sp-sgRNA, Addgene 65777) and the high-fidelity Cas9 (CMV-T7-humanSpCas9-HF1(N497A, R661A, Q695A, Q926A)-NLS-3xFLAG, Addgene 72247; Kleinstiver et al., 2016) were obtained from Addgene. Annealed oligos composing the guide RNAs were cloned into the BsmBI site of U6-BsmBIcassette-Sp-sgRNA. Neuro-2a cells were plated into a 12-well plate and transfected 48 hr later with 250 ng U6-BsmBIcassette-Sp-sgRNA (either empty vector or containing Fos^{RSINE} guide RNA) and 750 ng CMV-T7-human-SpCas9- HF1 using Lipofectamine 2000. The medium was changed 2–3 hr after transfection, and cells were harvested 48 hr later. For RNA analysis, cells were serum-starved 16 hr before adding forskolin (50 μM, 45 min). The guide RNA sequence used was GGTCATGCACTTGAGGTCATGGG (the last 3 letters are protospacer adjacent motif [PAM]).

Immuno-DNA FISH

Immuno-DNA FISH experiments were performed as described previously (Crepaldi et al., 2013) with some modifications. Briefly, cells were fixed for 10 min in 3% paraformaldehyde (PFA) in PBS, followed by permeabilization for 10 min in 0.5% Triton X-100 in PBS. After blocking with PBS+ (PBS plus 0.1% casein, 1% BSA, 0.2% fish skin gelatin) for 1 hr, coverslips were incubated overnight with Pol II-Ser5p (1:500, 4H8, Millipore 06-623) and GFP (1:2,000, Abcam ab13970) antibodies in PBS+. For detection, coverslips were incubated with anti-mouse Alexa Fluor 568 (1:1,000, Life Technologies) and anti-chicken Alexa Fluor 488 (1:1,000, Life Technologies) for 1 hr in PBS+. Post-fixation in 3% PFA in PBS (10 min) was followed by permeabilization in 0.1 M HCl and 0.7% Triton X-100 (10 min on ice) and by denaturation in 70% formamide in 2× saline sodium citrate (SSC) (80°C, 30 min). FISH hybridization with digoxigenin-labeled probes was carried out overnight at 42°C. The probes (bacterial artificial chromosome/clones [BACs] Fos RP24-233K8 and Csn2 RP23-110B6) were labeled with digoxigenin-deoxyuridine triphosphate (dUTP) using a nick translation kit (Roche), denatured (95°C, 5 min), and pre-annealed (37°C, 45 min) with Cot-1 DNA in hybridization buffer (50% formamide, 20% dextran sulfate, 2× SSC, and 1 mg/mL BSA) immediately before hybridization. FISH signals were amplified using sheep anti-digoxigenin fluorescein Fab fragments (1:50, Roche 11207741910) and fluorescein rabbit anti-sheep antibodies (1:100, Vector Laboratories FI-6000); DNA was counterstained with DAPI. Confocal images of neuronal nuclei were acquired using a Leica SPE3 confocal microscope. The co-localization threshold was set to 225 nm, corresponding to the distance at which the two smallest detectable objects overlap.

In Utero Electroporation

E13.5 pregnant mice were anesthetized with isoflurane in oxygen carrier (Abbot Laboratories), and the uterine horns were exposed through a small incision in the ventral peritoneum. Plasmid DNA solution (0.5–1.5 μg/μL), prepared using the EndoFree plasmid purification kit (QIAGEN), was mixed with 50 μM antisense LNA GapmeR (*in vivo*-ready, Exiqon) and 0.05% Fast Green (Sigma) and injected through the uterine wall into the lateral ventricles of the embryos using pulled borosilicate needles and a Femtojet microinjector (Eppendorf). Five electrical pulses were applied at 35 V (50-ms duration) across the uterine

wall at 950-ms intervals using 5-mm platinum Tweezertrodes (Harvard Apparatus) and an ECM-830 BTX square wave electroporator (Harvard Apparatus). The uterine horns were replaced in the abdominal cavity and the abdomen wall, and the skin was sutured. 48 hr after surgery, pregnant mice were sacrificed, and embryos were subjected to immunofluorescence to assess radial migration and expression of proliferation and laminar markers.

Radial Neural Migration Analysis

Embryos were electroporated *in utero* with the indicated GFP vectors, and analysis of radial migration was performed as described using ImageJ and an Excel macro (Nitarska et al., 2016). Images were acquired on an SP8 confocal microscope with Leica Application Suite Advanced Fluorescence (LAS AF) software using a 20× objective at 1,024 × 1,024 pixel resolution. Confocal images were run through a band-pass filter to segment and isolate cell-sized shapes, thresholded and segmented into 10 radial regions between the ventricle and the pial surface. Individual cell position along the radial axis was recorded and imported into Excel along with the coordinates of top (pial) and bottom (ventricle) boundaries obtained using ImageJ's Path Writer plugin. The distance and percentage of migrating cells in each area were calculated using an Excel macro.

DATA AND SOFTWARE AVAILABILITY

The accession number for the ChIP-seq data reported in this study is GEO: GSE75191.

SUPPLEMENTAL INFORMATION

Supplemental Information includes Supplemental Experimental Procedures, seven figures, and three tables and can be found with this article online at https://doi.org/10.1016/j.celrep.2017.11.019.

AUTHOR CONTRIBUTIONS

C.P., L.C., and A.R. conceived the project and designed the experiments. C.P., L.C., E.B., J.N., S.M.F., and A.C. performed the biochemical, cellular, and molecular biology experiments. L.C. performed the bioinformatics analyses. C.P., L.C., E.B., and A.R. wrote the paper, and all authors commented on the manuscript.

ACKNOWLEDGMENTS

We thank Robert White (University of York, York, UK) for the generous gift of the Pol III (Rpc155 subunit) antibody and Mike Hubank (UCL Genomics, London, UK) for assistance with sequencing. We thank Miranda Wilson (MRC-LMCB, UCL) for help and suggestions with the CRISPR-Cas9 experiments and Igor Ruiz De Los Mozos and Jernej Ule (The Crick Institute, UCL) for bioinformatic support. We are also grateful to Hamish Crerar, Alexi Nott, Adolfo Saiardi, and Paolo Salomoni for critical reading of the manuscript and to all members of the Riccio lab for helpful discussions. This work was supported by an MRC Senior Non-clinical Fellowship SNCF G0802010 (to A.R.), a Wellcome Trust Investigator Award 103717/Z/14/Z (to A.R.), a Marie Skłodowska-Curie Postdoctoral Fellowship 702337 (to E.B.), and an MRC LMCB Core Award MC_U12266B.

Received: June 20, 2016
Revised: June 30, 2017
Accepted: November 2, 2017
Published: December 5, 2017

REFERENCES

Allen, T.A., Von Kaenel, S., Goodrich, J.A., and Kugel, J.F. (2004). The SINE-encoded mouse B2 RNA represses mRNA transcription in response to heat shock. Nat. Struct. Mol. Biol. *11*, 816–821.

Athanasiadis, A., Rich, A., and Maas, S. (2004). Widespread A-to-I RNA editing of Alu-containing mRNAs in the human transcriptome. PLoS Biol. *2*, e391.

Barski, A., Chepelev, I., Liko, D., Cuddapah, S., Fleming, A.B., Birch, J., Cui, K., White, R.J., and Zhao, K. (2010). Pol II and its associated epigenetic marks are present at Pol III-transcribed noncoding RNA genes. Nat. Struct. Mol. Biol. *17*, 629–634.

Boyle, A.P., Davis, S., Shulha, H.P., Meltzer, P., Margulies, E.H., Weng, Z., Furey, T.S., and Crawford, G.E. (2008). High-resolution mapping and characterization of open chromatin across the genome. Cell *132*, 311–322.

Britten, R.J., and Davidson, E.H. (1969). Gene regulation for higher cells: a theory. Science *165*, 349–357.

Chen, C., Ara, T., and Gautheret, D. (2009). Using Alu elements as polyadenylation sites: A case of retroposon exaptation. Mol. Biol. Evol. *26*, 327–334.

Collis, P., Antoniou, M., and Grosveld, F. (1990). Definition of the minimal requirements within the human beta-globin gene and the dominant control region for high level expression. EMBO J. *9*, 233–240.

Cook, P.R. (2010). A model for all genomes: the role of transcription factories. J. Mol. Biol. *395*, 1–10.

Crepaldi, L., Policarpi, C., Coatti, A., Sherlock, W.T., Jongbloets, B.C., Down, T.A., and Riccio, A. (2013). Binding of TFIIIC to sine elements controls the relocation of activity-dependent neuronal genes to transcription factories. PLoS Genet. *9*, e1003699.

Dieci, G., Fiorino, G., Castelnuovo, M., Teichmann, M., and Pagano, A. (2007). The expanding RNA polymerase III transcriptome. Trends Genet. *23*, 614–622.

Faulkner, G.J., Kimura, Y., Daub, C.O., Wani, S., Plessy, C., Irvine, K.M., Schroder, K., Cloonan, N., Steptoe, A.L., Lassmann, T., et al. (2009). The regulated retrotransposon transcriptome of mammalian cells. Nat. Genet. *41*, 563–571.

Flavell, S.W., and Greenberg, M.E. (2008). Signaling mechanisms linking neuronal activity to gene expression and plasticity of the nervous system. Annu. Rev. Neurosci. *31*, 563–590.

Frank, C.L., Liu, F., Wijayatunge, R., Song, L., Biegler, M.T., Yang, M.G., Vockley, C.M., Safi, A., Gersbach, C.A., Crawford, G.E., and West, A.E. (2015). Regulation of chromatin accessibility and Zic binding at enhancers in the developing cerebellum. Nat. Neurosci. *18*, 647–656.

Gomez, N.C., Hepperla, A.J., Dumitru, R., Simon, J.M., Fang, F., and Davis, I.J. (2016). Widespread Chromatin Accessibility at Repetitive Elements Links Stem Cells with Human Cancer. Cell Rep. *17*, 1607–1620.

Greenberg, M.E., Ziff, E.B., and Greene, L.A. (1986). Stimulation of neuronal acetylcholine receptors induces rapid gene transcription. Science *234*, 80–83.

Heintzman, N.D., Hon, G.C., Hawkins, R.D., Kheradpour, P., Stark, A., Harp, L.F., Ye, Z., Lee, L.K., Stuart, R.K., Ching, C.W., et al. (2009). Histone modifications at human enhancers reflect global cell-type-specific gene expression. Nature *459*, 108–112.

Hevner, R.F., Shi, L., Justice, N., Hsueh, Y., Sheng, M., Smiga, S., Bulfone, A., Goffinet, A.M., Campagnoni, A.T., and Rubenstein, J.L. (2001). Tbr1 regulates differentiation of the preplate and layer 6. Neuron *29*, 353–366.

Huda, A., Mariño-Ramírez, L., and Jordan, I.K. (2010). Epigenetic histone modifications of human transposable elements: genome defense versus exaptation. Mob. DNA *1*, 2.

Ichiyanagi, K. (2013). Epigenetic regulation of transcription and possible functions of mammalian short interspersed elements, SINEs. Genes Genet. Syst. *88*, 19–29.

Kaikkonen, M.U., Spann, N.J., Heinz, S., Romanoski, C.E., Allison, K.A., Stender, J.D., Chun, H.B., Tough, D.F., Prinjha, R.K., Benner, C., and Glass, C.K. (2013). Remodeling of the enhancer landscape during macrophage activation is coupled to enhancer transcription. Mol. Cell *51*, 310–325.

Kim, D.D.Y., Kim, T.T.Y., Walsh, T., Kobayashi, Y., Matise, T.C., Buyske, S., and Gabriel, A. (2004). Widespread RNA editing of embedded alu elements in the human transcriptome. Genome Res. *14*, 1719–1725.

Kim, T.-K., Hemberg, M., Gray, J.M., Costa, A.M., Bear, D.M., Wu, J., Harmin, D.A., Laptewicz, M., Barbara-Haley, K., Kuersten, S., et al. (2010). Widespread transcription at neuronal activity-regulated enhancers. Nature *465*, 182–187.

Kleinstiver, B.P., Pattanayak, V., Prew, M.S., Tsai, S.Q., Nguyen, N.T., Zheng, Z., and Joung, J.K. (2016). High-fidelity CRISPR-Cas9 nucleases with no detectable genome-wide off-target effects. Nature *529*, 490–495.

Koch, F., Fenouil, R., Gut, M., Cauchy, P., Albert, T.K., Zacarias-Cabeza, J., Spicuglia, S., de la Chapelle, A.L., Heidemann, M., Hintermair, C., et al. (2011). Transcription initiation platforms and GTF recruitment at tissue-specific enhancers and promoters. Nat. Struct. Mol. Biol. *18*, 956–963.

Kolovos, P., Knoch, T.A., Grosveld, F.G., Cook, P.R., and Papantonis, A. (2012). Enhancers and silencers: an integrated and simple model for their function. Epigenetics Chromatin *5*, 1.

Lam, M.T.Y., Cho, H., Lesch, H.P., Gosselin, D., Heinz, S., Tanaka-Oishi, Y., Benner, C., Kaikkonen, M.U., Kim, A.S., Kosaka, M., et al. (2013). Rev-Erbs repress macrophage gene expression by inhibiting enhancer-directed transcription. Nature *498*, 511–515.

Lam, M.T.Y., Li, W., Rosenfeld, M.G., and Glass, C.K. (2014). Enhancer RNAs and regulated transcriptional programs. Trends Biochem. Sci. *39*, 170–182.

Levanon, E.Y., Eisenberg, E., Yelin, R., Nemzer, S., Hallegger, M., Shemesh, R., Fligelman, Z.Y., Shoshan, A., Pollock, S.R., Sztybel, D., et al. (2004). Systematic identification of abundant A-to-I editing sites in the human transcriptome. Nat. Biotechnol. *22*, 1001–1005.

Li, W., Notani, D., Ma, Q., Tanasa, B., Nunez, E., Chen, A.Y., Merkurjev, D., Zhang, J., Ohgi, K., Song, X., et al. (2013). Functional roles of enhancer RNAs for oestrogen-dependent transcriptional activation. Nature *498*, 516–520.

Lunyak, V.V., Prefontaine, G.G., Nunez, E., Cramer, T., Ju, B.-G., Ohgi, K.A., Hutt, K., Roy, R., García-Díaz, A., Zhu, X., et al. (2007). Developmentally regulated activation of a SINE B2 repeat as a domain boundary in organogenesis. Science *317*, 248–251.

Ma, D.K., Jang, M.-H., Guo, J.U., Kitabatake, Y., Chang, M.-L., Pow-Anpongkul, N., Flavell, R.A., Lu, B., Ming, G.-L., and Song, H. (2009). Neuronal activity-induced Gadd45b promotes epigenetic DNA demethylation and adult neurogenesis. Science *323*, 1074–1077.

Malik, A.N., Vierbuchen, T., Hemberg, M., Rubin, A.A., Ling, E., Couch, C.H., Stroud, H., Spiegel, I., Farh, K.K.-H., Harmin, D.A., and Greenberg, M.E. (2014). Genome-wide identification and characterization of functional neuronal activity-dependent enhancers. Nat. Neurosci. *17*, 1330–1339.

Mariner, P.D., Walters, R.D., Espinoza, C.A., Drullinger, L.F., Wagner, S.D., Kugel, J.F., and Goodrich, J.A. (2008). Human Alu RNA is a modular transacting repressor of mRNA transcription during heat shock. Mol. Cell *29*, 499–509.

Melo, C.A., Drost, J., Wijchers, P.J., van de Werken, H., de Wit, E., Oude Vrielink, J.A., Elkon, R., Melo, S.A., Léveillé, N., Kalluri, R., et al. (2013). eRNAs are required for p53-dependent enhancer activity and gene transcription. Mol. Cell *49*, 524–535.

Moqtaderi, Z., and Struhl, K. (2004). Genome-wide occupancy profile of the RNA polymerase III machinery in Saccharomyces cerevisiae reveals loci with incomplete transcription complexes. Mol. Cell. Biol. *24*, 4118–4127.

Moqtaderi, Z., Wang, J., Raha, D., White, R.J., Snyder, M., Weng, Z., and Struhl, K. (2010). Genomic binding profiles of functionally distinct RNA polymerase III transcription complexes in human cells. Nat. Struct. Mol. Biol. *17*, 635–640.

Mousavi, K., Zare, H., Dell'orso, S., Grontved, L., Gutierrez-Cruz, G., Derfoul, A., Hager, G.L., and Sartorelli, V. (2013). eRNAs promote transcription by establishing chromatin accessibility at defined genomic loci. Mol. Cell *51*, 606–617.

Muotri, A.R., Marchetto, M.C.N., Coufal, N.G., and Gage, F.H. (2007). The necessary junk: new functions for transposable elements. Hum. Mol. Genet. *16*, R159–R167.

Nakanishi, A., Kobayashi, N., Suzuki-Hirano, A., Nishihara, H., Sasaki, T., Hirakawa, M., Sumiyama, K., Shimogori, T., and Okada, N. (2012). A SINE-derived element constitutes a unique modular enhancer for mammalian diencephalic Fgf8. PLoS ONE *7*, e43785.

Nitarska, J., Smith, J.G., Sherlock, W.T., Hillege, M.M.G., Nott, A., Barshop, W.D., Vashisht, A.A., Wohlschlegel, J.A., Mitter, R., and Riccio, A. (2016). A Functional Switch of NuRD Chromatin Remodeling Complex Subunits Regulates Mouse Cortical Development. Cell Rep. *17*, 1683–1698.

Ohnishi, Y., Totoki, Y., Toyoda, A., Watanabe, T., Yamamoto, Y., Tokunaga, K., Sakaki, Y., Sasaki, H., and Hohjoh, H. (2012). Active role of small non-coding RNAs derived from SINE/B1 retrotransposon during early mouse development. Mol. Biol. Rep. *39*, 903–909.

Oler, A.J., Alla, R.K., Roberts, D.N., Wong, A., Hollenhorst, P.C., Chandler, K.J., Cassiday, P.A., Nelson, C.A., Hagedorn, C.H., Graves, B.J., and Cairns, B.R. (2010). Human RNA polymerase III transcriptomes and relationships to Pol II promoter chromatin and enhancer-binding factors. Nat. Struct. Mol. Biol. *17*, 620–628.

Orioli, A., Pascali, C., Pagano, A., Teichmann, M., and Dieci, G. (2012). RNA polymerase III transcription control elements: themes and variations. Gene *493*, 185–194.

Raha, D., Wang, Z., Moqtaderi, Z., Wu, L., Zhong, G., Gerstein, M., Struhl, K., and Snyder, M. (2010). Close association of RNA polymerase II and many transcription factors with Pol III genes. Proc. Natl. Acad. Sci. USA *107*, 3639–3644.

Rebollo, R., Romanish, M.T., and Mager, D.L. (2012). Transposable elements: an abundant and natural source of regulatory sequences for host genes. Annu. Rev. Genet. *46*, 21–42.

Rieder, D., Trajanoski, Z., and McNally, J.G. (2012). Transcription factories. Front. Genet. *3*, 221.

Roeder, R.G. (1996). Nuclear RNA polymerases: role of general initiation factors and cofactors in eukaryotic transcription. Methods Enzymol. *273*, 165–171.

Sasaki, T., Nishihara, H., Hirakawa, M., Fujimura, K., Tanaka, M., Kokubo, N., Kimura-Yoshida, C., Matsuo, I., Sumiyama, K., Saitou, N., et al. (2008). Possible involvement of SINEs in mammalian-specific brain formation. Proc. Natl. Acad. Sci. USA *105*, 4220–4225.

Schaukowitch, K., Joo, J.-Y., Liu, X., Watts, J.K., Martinez, C., and Kim, T.-K. (2014). Enhancer RNA facilitates NELF release from immediate early genes. Mol. Cell *56*, 29–42.

Sheng, M., McFadden, G., and Greenberg, M.E. (1990). Membrane depolarization and calcium induce c-fos transcription via phosphorylation of transcription factor CREB. Neuron *4*, 571–582.

Su, M., Han, D., Boyd-Kirkup, J., Yu, X., and Han, J.-D.J. (2014). Evolution of Alu elements toward enhancers. Cell Rep. *7*, 376–385.

Sultan, F.A., Wang, J., Tront, J., Liebermann, D.A., and Sweatt, J.D. (2012). Genetic deletion of Gadd45b, a regulator of active DNA demethylation, enhances long-term memory and synaptic plasticity. J. Neurosci. *32*, 17059–17066.

Sutherland, H., and Bickmore, W.A. (2009). Transcription factories: gene expression in unions? Nat. Rev. Genet. *10*, 457–466.

Sweatt, J.D. (2016). Neural plasticity and behavior: sixty years of conceptual advances. J. Neurochem. *139*, 179–199.

Tashiro, K., Teissier, A., Kobayashi, N., Nakanishi, A., Sasaki, T., Yan, K., Tarabykin, V., Vigier, L., Sumiyama, K., Hirakawa, M., et al. (2011). A mammalian conserved element derived from SINE displays enhancer properties recapitulating Satb2 expression in early-born callosal projection neurons. PLoS ONE *6*, e28497.

Telese, F., Ma, Q., Perez, P.M., Notani, D., Oh, S., Li, W., Comoletti, D., Ohgi, K.A., Taylor, H., and Rosenfeld, M.G. (2015). LRP8-Reelin-Regulated Neuronal Enhancer Signature Underlying Learning and Memory Formation. Neuron *86*, 696–710.

Velazquez, F.N., Prucca, C.G., Etienne, O., D'Astolfo, D.S., Silvestre, D.C., Boussin, F.D., and Caputto, B.L. (2015). Brain development is impaired in c-fos -/- mice. Oncotarget *6*, 16883–16901.

Wang, D., Garcia-Bassets, I., Benner, C., Li, W., Su, X., Zhou, Y., Qiu, J., Liu, W., Kaikkonen, M.U., Ohgi, K.A., et al. (2011). Reprogramming transcription by distinct classes of enhancers functionally defined by eRNA. Nature *474*, 390–394.

West, A.E., and Greenberg, M.E. (2011). Neuronal activity-regulated gene transcription in synapse development and cognitive function. Cold Spring Harb. Perspect. Biol. *3*, a005744.

White, R.J. (2011). Transcription by RNA polymerase III: more complex than we thought. Nat. Rev. Genet. *12*, 459–463.

Wu, L., Pan, J., Thoroddsen, V., Wysong, D.R., Blackman, R.K., Bulawa, C.E., Gould, A.E., Ocain, T.D., Dick, L.R., Errada, P., et al. (2003). Novel small-molecule inhibitors of RNA polymerase III. Eukaryot. Cell *2*, 256–264.

Yankulov, K., Yamashita, K., Roy, R., Egly, J.M., and Bentley, D.L. (1995). The transcriptional elongation inhibitor 5,6-dichloro-1-beta-D-ribofuranosylbenzimidazole inhibits transcription factor IIH-associated protein kinase. J. Biol. Chem. *270*, 23922–23925.

Zentner, G.E., Tesar, P.J., and Scacheri, P.C. (2011). Epigenetic signatures distinguish multiple classes of enhancers with distinct cellular functions. Genome Res. *21*, 1273–1283.